IET Microwaves, Antennas & Propagation

The Institution of Engineering and Technology WILEY

ORIGINAL RESEARCH PAPER

Four-dimensional relativistic scattering of electromagnetic waves from an arbitrary collection of moving lossy dielectric spheres

Hamed Radpour[1] | Ali Pourziad[2] | Kamal Sarabandi[3]

[1]Department of Electrical Engineering, Korea Advanced Institute of Science & Technology (KAIST), Daejeon, South Korea

[2]Department of Electrical Engineering & Computer Science, University of Tabriz, Tabriz, Iran

[3]Department of Electrical Engineering, University of Michigan, Ann Arbor, MI, USA

Correspondence

Hamed Radpour, Department of Electrical Engineering, Korea Advanced Institute of Science & Technology (KAIST), Daejeon, South Korea.
Email: hradpour@kaist.ac.kr

Abstract

Four-dimensional (4D) relativistic scattering of electromagnetic waves from an arbitrary collection of uniformly translational moving lossy dielectric spheres is discussed. Two reference frames, four 4D coordinate systems and Lorentz transformation are used to obtain the scattered electromagnetic fields. The direct scattering of the spheres and their interactions are considered with a novel approach. The introduced method is straightforward and the analytical relations for the fields are achieved. To check the validity of the proposed method, different examples for both stationary and moving scatterers are investigated. The effects of key parameters such as the size, material, velocity, number, position of the spheres and also the frequency of the incident wave are discussed. The derived scattered fields are valid for low, medium and high velocities but according to practical applications low and moderate velocities are highlighted in numerical results.

1 | INTRODUCTION

A very interesting subject in electromagnetics is the scattering of electromagnetic (EM) waves from moving objects which has been investigated by researchers over the last century. From the standpoint of applications, for low and moderate speed cases, it can be used to calculate the attenuation and transmission of EM waves for rainy, snowy and dusty mediums, which is very important in meteorology, satellite communications, environmental issues, radar applications and remotely sensed data. Furthermore, for the profile of high-speed objects, it has applications in the understanding of scattering by relativistically moving interstellar dust grains [1], moving plasma columns [2–4] and mass flows in pneumatic pipes [5].

The important properties of objects such as shape, material, and velocity could be obtained by processing the scattered fields, which is known as inverse scattering. Furthermore, with post-processing, other significant practical characteristics of a collection of objects such as scattering, extinction and absorption cross-sections could be derived. The main challenge in random and multiple scattering is

obtaining the scattered fields from a collection of moving scatterers. In this case, 4 four-dimensional (4D) coordinate systems for the rest and moving frames and Special Theory of Relativity (STR) should be considered which causes mathematical difficulties.

Electromagnetic scattering of a translational moving body with STR, which was first introduced by Einstein in 1905 [6], has been used for a moving perfectly reflecting mirror [7,8]. By applying STR, EM scattered waves for different moving shapes such as dielectric medium [9,10] cylinder [11–15], conducting sphere [16], electrically small chiral sphere [17], small particle [18], perfectly conducting flat plate [19], rough surface [20], arbitrary obstacle [21–27], wedge [28,29] and half-plane [30–32] have been derived. Also, scattering characteristics (scattering cross-section, extinction and absorption) for a uniformly moving object [33] and a moving concentrically layered sphere [34] are discussed. The back-scattered signal by a uniformly moving sphere considering the incident wave to be a pulsed plane wave, is investigated [35]. All foregoing works discuss only one moving object whereas practical applications mostly deal with a collection of many moving random objects. In that case, not only

investigation on the relativistic translational motion of the individual object is required, the mutual interactions of the moving objects also have significant effects, which make the solution more complicated.

Time-domain scattered fields from an arbitrary collection of uniformly translational moving lossy-dielectric spheres are calculated in the far-field region. The size, material, velocity, number, position of the spheres and the frequency of the incident wave can be selected arbitrarily, which makes studying of effective parameters possible. By considering the intrinsic inaccuracies of using numerical techniques, such as the finite-difference–time-domain method (FDTD) and Lorentz precise integration time-domain method (Lorentz-PITD), for a moving object [36–42], here the STR and Mie theory [43–46] are employed. Also, other kinds of motions for an individual object such as rotational [47–51] and vibrational [52–54] have been investigated, but, here the translational motion is of interest.

2 | FORMULATION OF THE PROBLEM

A collection of uniformly translational moving spheres of radius a, a complex refractive index of $n = n' + jn''$ and a constant velocity of $\vec{\nu} = v\hat{z}$ moving along the z-direction is considered. Four 4D coordinate systems (three dimensions are associated with the position and one with the time) are considered regarding the rest and moving frames which are denoted with K and K', respectively, as shown in Figure 1. In the rest frame, the spheres appear to be moving and in the moving frame, the spheres seem to be stationary.

To synchronize times, K and K' are considered to coincide at time $t = t' = 0$. Each frame has two spatial coordinate systems. To characterize and solve the whole problem, Cartesian (x,y,z) and spherical (r, θ, φ) coordinate systems are considered for the rest frame (K) and similarly, the prime forms (x',y',z') and (r', θ', φ') are chosen to indicate the quantities in the moving frame (K'). Considering that all spheres are moving in the rest frame, it would be more appropriate to transform the problem to the moving frame. In other words, the problem is solved in K' and then the resulting scattered fields transformed back into K. The incident wave and the observation point are given in the K frame. According to symmetry characteristics of spheres, without losing generality, an incident plane wave is considered to propagate in the negative $x\hat{}$ direction[1] and has a polarization in the y direction which can be expressed in the rest frame by:

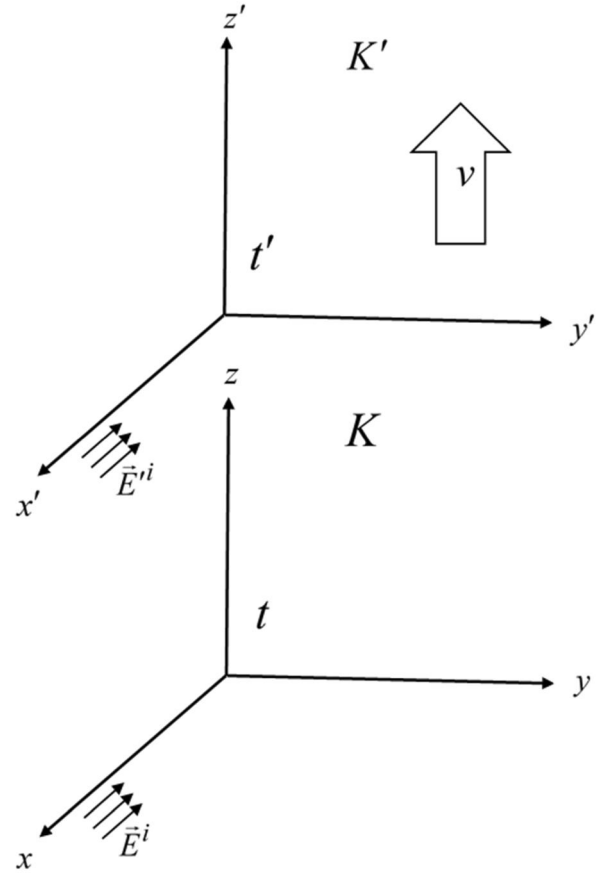$$\vec{E}^i = E^i e^{-jkx}\hat{y}, \vec{H}^i = -\frac{1}{\eta}\hat{x} \times \vec{E}^i \quad (1)$$

FIGURE 1 Two reference frames for relative motion

where η is the intrinsic impedance of the free space and k is the wave number in the rest frame.

2.1 | Electromagnetic scattering from a moving sphere:

At time $t = 0$, the coordinates of the ith moving sphere is represented by (x_{i0}, y_{i0}, z_{i0}). Moreover, τ is the time when the ith sphere scatters a spherical wavefront and r_i is the instantaneous distance between the ith moving sphere and the observation point (x_p, y_p, z_p), as shown in Figure 2. So the position of this sphere in the rest frame can be expressed by $(x_i, y_i, z_i, t) = (x_{i0}, y_{i0}, z_{i0} + v\tau, \tau)$ and the angle θ_i is defined as:

$$\cos \theta_i = \frac{z_p - z_{i0} - v\tau}{r_i} \quad (2)$$

$$r_i = \left[(x_p - x_i)^2 + (y_p - y_i)^2 + (z_p - z_{i0} - v\tau)^2 \right]^{\frac{1}{2}} \quad (3)$$

In orther to associate K and K' using the Lorentz transformation [7, 8]

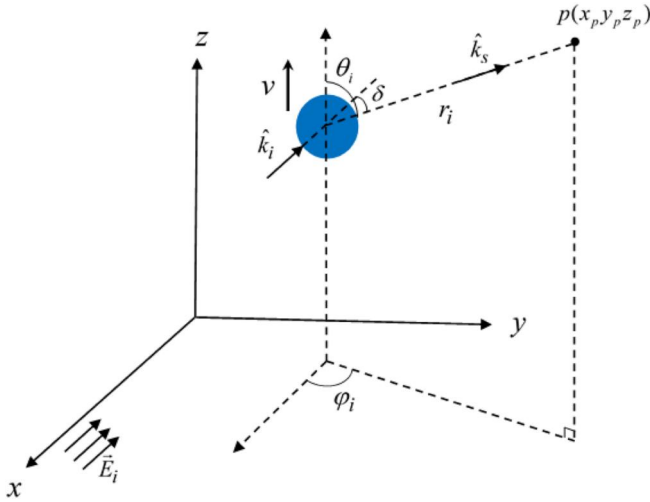[1]Throughout this article $e^{-j\omega t}$ used to transform to the time-harmonic fields.

FIGURE 2 Scattering configuration and angles for a sphere moving with velocity v along the z-direction

$$x_i' = x_i; \quad y_i' = y_i; \quad z_i' = \frac{z_i - v\tau}{\sqrt{1 - \beta^2}}; \quad t' = \frac{t - \left(\frac{v}{c^2}\right)z_i}{\sqrt{1 - \beta^2}} \quad (4)$$

where $\beta = v/c$ and c is the speed of light in free space. The components of the spherical coordinate system in K' can be written as [7,8]:

$$r_i' = \frac{1 - \beta \cos\theta_i}{\sqrt{1 - \beta^2}} r_i \quad (5)$$

$$\cos\theta_i' = \frac{\cos\theta_i - \beta}{1 - \beta\cos\theta_i} \; ; \; \sin\theta_i' = \frac{\sin\theta_i\sqrt{1 - \beta^2}}{1 - \beta\cos\theta_i} \quad (6)$$

$$\cos\varphi_i' = \frac{x_p' - x_i'}{r_i'\sin\theta_i'} \; ; \; \sin\varphi_i' = \frac{y_p' - y_i'}{r_i'\sin\theta_i'} \; ; \quad \varphi_i' = \varphi_i \quad (7)$$

The incident plane wave is transformed into the moving frame [7,16]:

$$\vec{E}^{'i} = \frac{1}{\sqrt{1 - \beta^2}} E^i e^{-jk'x'} \hat{y} \quad (8)$$

$$k' = \frac{k}{\sqrt{1 - \beta^2}} \quad (9)$$

By applying Mie theory to the incident field[2] for the far-field region ($k'r' \gg 1$) in the moving frame, the direct scattered field can be derived as

$$E_\theta'^{ds} = \frac{1}{\sqrt{1 - \beta^2}}\left[S_1(\delta')\sin\varphi_i' \cos\theta_i'\right.$$

$$\left. + 0.25 S_2(\delta')\sin 2\theta_i' \sin 2\varphi_i'\right]\frac{je^{jk'r_i'}}{k'r_i' X'^2} \quad (10)$$

$$E_\varphi'^{ds} = \frac{1}{\sqrt{1 - \beta^2}}\left[S_1(\delta')\cos^2\theta_i' \cos\varphi_i'\right.$$

$$\left. - S_2(\delta')\sin 2\varphi_i' \sin\theta_i'\right]\frac{je^{jk'r_i'}}{k'r_i' X'^2} \quad (11)$$

with $X' = (1 - \sin^2\theta_i' \cos^2\varphi_i')^{\frac{1}{2}}$ and δ' is the angle between the incident direction ($\hat{k}_i'$) and the scattering direction ($\hat{k}_s'$). The scattering amplitude matrix coefficients for Mie theory [45] can be stated as

$$S_1(\delta) = \sum_{n=1}^{\infty} \frac{2n+1}{n(n+1)}[a_n\pi_n(\cos\delta) + b_n\tau_n(\cos\delta)]$$
$$S_2(\delta) = \sum_{n=1}^{\infty} \frac{2n+1}{n(n+1)}[a_n\tau_n(\cos\delta) + b_n\pi_n(\cos\delta)] \quad (12a)$$

where

$$\pi_n(\cos\delta) = -\frac{P_n^1(\cos\delta)}{\sin\delta}$$

$$\tau_n(\cos\delta) = -\frac{dP_n^1(\cos\delta)}{d\delta} \quad (12b)$$

$$a_n = \frac{k_p^2 a^2 j_n(k_p a)\left[kaj_n(ka)\right]' - k^2 a^2 j_n(ka)\left[k_p a j_n(k_p a)\right]'}{k_p^2 a^2 j_n(k_p a)\left[kah_n(ka)\right]' - k^2 a^2 h_n(ka)\left[k_p a j_n(k_p a)\right]'}$$

$$b_n = \frac{j_n(k_p a)\left[kaj_n(ka)\right]' - j_n(ka)\left[k_p a j_n(k_p a)\right]'}{j_n(k_p a)\left[kah_n(ka)\right]' - h_n(ka)\left[k_p a j_n(k_p a)\right]'}$$

$$(12c)$$

where a is the radius of the sphere, a_n, b_n are the Mie scattering coefficients, j_n, h_n are the spherical Bessel and Hankel functions of the first kind, respectively, P_n is the associated Legendre function and prime is the notation for derivation.

To transform back to the stationary frame, the following relations are used [7].

$$E_\theta^{ds} = \frac{\sqrt{1 - \beta^2}}{1 - \beta\cos\theta_i} E_\theta'^{ds} \; ; \quad E_\varphi^{ds} = \frac{\sqrt{1 - \beta^2}}{1 - \beta\cos\theta_i} E_\varphi'^{ds} \quad (13)$$

Hence, the time-harmonic expressions[3] for E_θ^{ds} and $E_\varphi'^{ds}$ can be written according to Equations (10), (11), and (13) as

---

[2]For the convenience amplitude of the incident field is considered to be 1 V/m.

[3]For the sake of simplicity the *Real*{.}operation is not represented.

$$E_\theta{}^{ds} = \frac{1}{1 - \beta \cos \theta_i} \left[\frac{1}{X'^2} \left(S_1(\delta') \sin\varphi'_i \cos\theta'_i \right. \right.$$
$$\left. \left. + 0.25 S_2(\delta') \sin 2\theta'_i \sin 2\varphi'_i \right) \right] \frac{j e^{jk'(r'_i - ct')}}{k' r'_i} \quad (14)$$

$$E_\varphi{}^{ds} = \frac{1}{1 - \beta \cos \theta_i} \left[\frac{1}{X'^2} \left(S_1(\delta') \cos{}^2\theta'_i \cos\varphi'_i \right. \right.$$
$$\left. \left. - S_2(\delta') \sin{}^2\varphi'_i \sin\theta'_i \right) \right] \frac{j e^{jk'(r'_i - ct')}}{k' r'_i} \quad (15)$$

To represent the phase factor $(e^{jk'(r'_i - ct')})$ of the obtained scattered fields in an unprimed form and to relate it with τ it should be noted that

$$r'_i = c(t' - \tau') \ and \ jk'(r'_i - ct') = -jk' c\tau \sqrt{1 - \beta^2} \quad (16)$$

By applying Equations (16) and (9) to (14) and (15), the time-harmonic direct scattered fields in the rest frame could be expressed by:

$$E_\theta{}^{ds} = \frac{1 - \beta^2}{(1 - \beta \cos \theta_i)} \left[\frac{1}{X'^2} \left(S_1(\delta') \sin\varphi'_i \cos\theta'_i \right. \right.$$
$$\left. \left. + 0.25 S_2(\delta') \sin 2\theta'_i \sin 2\varphi'_i \right) \right] \frac{j e^{-jkc\tau}}{k r_i} \quad (17)$$

$$E_\varphi{}^{ds} = \frac{1 - \beta^2}{1 - \beta \cos \theta_i} \left[\frac{1}{X'^2} \left(S_1(\delta') \cos{}^2\theta'_i \cos\varphi'_i \right. \right.$$
$$\left. \left. - S_2(\delta') \sin{}^2\varphi'_i \sin\theta'_i \right) \right] \frac{j e^{-jkc\tau}}{k r_i} \quad (18)$$

$$\vec{H}^{ds} = \frac{1}{\eta} \hat{r} \times (E_\theta{}^{ds} \hat{\theta} + E_\varphi{}^{ds} \hat{\varphi}) \quad (19)$$

It is important to state that although these direct scattered fields components are functions of τ, they represent the scattered fields in the observation point at time $t = \tau + r_i/c$.

2.2 | Secondary electromagnetic scattering fields from two spheres configurations

In this section, two moving spheres are considered and the problem is to evaluate the secondary scattered fields. The secondary scattered fields are the fields scattered from a moving sphere, when illuminated by a primary scattered field from another moving sphere. Assuming that ith and jth spheres are moving along the z-direction, as represented
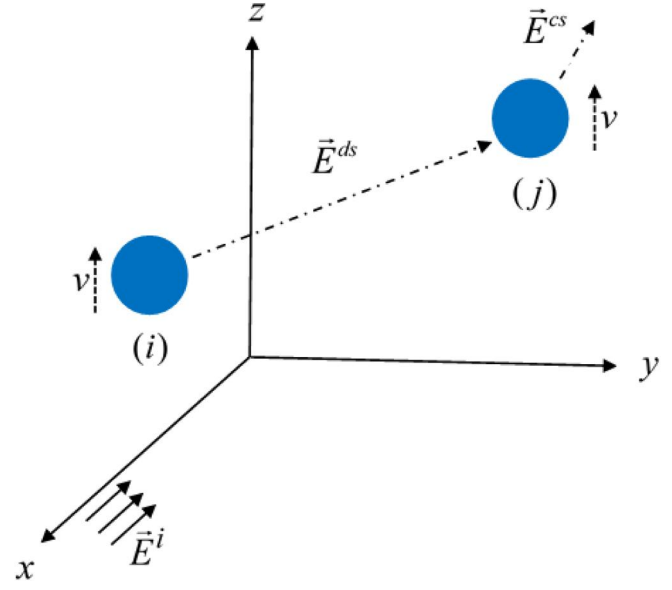

FIGURE 3 Two moving spheres with the direct and coupling scattered fields

in Figure 3, their positions in the K frame can be expressed by

$$(x_i, \ y_i, \ z_i, t) = (x_{i0}, \ y_{i0}, \ z_{i0} + \ v\tau, \tau)$$
$$(x_j, \ y_j, \ z_j, t) = (x_{j0}, \ y_{j0}, \ z_{j0} + \ v\tau, \tau) \quad (20)$$

The incident field in Equation (1) is upon the ith sphere and this sphere scatters a field which illuminates the jth sphere, then the jth sphere scatters a field which would be calculated. Since these two spheres move with an equal velocity and have an identical direction of motion, they appear stationary to each other in the moving frame; therefore, the secondary scattered fields can be called coupling fields. It is assumed that the jth sphere is in the far-field region of the ith sphere. If the distance between the two spheres represented by d_{ij} and the radius of the ith sphere denoted by a_i then the far-field condition mathematically can be stated as

$$d_{ij} \geq \frac{8a_i{}^2}{\lambda} \quad (21)$$

According to the length–contraction property of STR, it can be written that

$$d'_{ij} = \frac{1 - \beta \cos \theta_{ij}}{\sqrt{1 - \beta^2}} d_{ij}, r'_j = \frac{1 - \beta \cos \theta_j}{\sqrt{1 - \beta^2}} r_j \quad (22)$$

where r_j is considered as the instantaneous distance between sphere number j and the observation point (x_p, y_p, z_p) in the K frame.

The parameters $(\theta_{ij}, \varphi_{ij})$ and (θ_j, φ_j) are defined as

$$\cos \theta_{ij} = \frac{1}{d_{ij}}(z_j - z_i) \tag{23}$$

$$\cos \varphi_{ij} = \frac{1}{d_{ij} \sin \theta_{ij}}(x_j - x_i); \sin \varphi_{ij} = \frac{1}{d_{ij} \sin \theta_{ij}}(y_j - y_i) \tag{24}$$

$$\cos \theta_j = \frac{1}{r_j}(z_p - z_{j0} - v\tau) \tag{25}$$

$$\cos \varphi_j = \frac{1}{r_j \sin \theta_j}(x_p - x_j); \sin \varphi_j = \frac{1}{r_j \sin \theta_j}(y_p - y_j) \tag{26}$$

The prime forms of $(\theta_{ij}, \varphi_{ij})$ and (θ_j, φ_j) in moving frame can be obtained in a similar way to Equations (6) and (7).

The coupling fields would be calculated by applying Mie theory in two levels and transformations between stationary and moving frames would be employed.

The parameters S_{1i}, S_{2i}, S_{1j} and S_{2j} construct the scattering amplitude matrices that are used to calculate the primary and secondary scattered fields. The parameters S_{1i}, S_{2i} which are used for evaluation of the scattered fields from the ith sphere could be obtained with direct replacement of δ'_i in Equations (12a) and (12b) and S_{1j}, S_{2j} are related to the jth sphere that could be achieved by replacing δ'_{ij} in Equations (12a) and (12b).

$$\cos(\delta'_i) = -\sin\theta'_{ij}\cos\varphi'_{ij} \tag{27a}$$

$$\cos(\delta'_{ij}) = \frac{1}{d'_{ij}r'_j}\left[\left(x'_{pj}\left(x'_j - x'_i\right) + y'_{pj}\left(y'_j - y'_i\right)\right. \right.$$
$$\left.\left. + z'_{pj}(z'_j - z'_i)\right]\right. \tag{27b}$$

The parameters $\hat{k}_i$ and $\hat{k}_s$ are incident and scattered field propagation directions, respectively, associated with the jth sphere. Therefore $(\hat{1}_i, \hat{2}_i, \hat{k}_i)$ and $(\hat{1}_s, \hat{2}_s, \hat{k}_s)$ are the orthonormal unit systems [45] to characterize scattering by the jth sphere which can be defined as

$$x'_{pj} = x'_p - x'_j; y'_{pj} = y'_p - y'_j; z'_{pj} = z'_p - z'_j$$

$$\hat{k}'_i = \frac{1}{d'_{ij}}\left[x'_{pj}\hat{x}' + y'_{pj}\hat{y}' + z'_{pj}\hat{z}'\right], \hat{k}'_s = r'_j$$

$$\hat{1}'_i = \hat{1}'_s = \frac{\hat{k}'_s \times \hat{k}'_i}{|\hat{k}'_s \times \hat{k}'_i|} = \frac{1}{N'}[\hat{\theta}L'_4 + \hat{\varphi}L'_6] \tag{28}$$

$$\hat{2}'_i = \hat{k}'_i \times \hat{1}'_i = -\frac{1}{d'_{ij}N'}[\hat{\theta}L'_5 + \hat{\varphi}L'_6]$$

$$\hat{2}'_s = \hat{k}'_s \times \hat{1}'_s = \frac{1}{N'}[-\hat{\theta}L'_4 + \hat{\varphi}L'_3]$$

where

$$u'_1 = x'_{pj}\left(y'_j - y'_i\right) - y'_{pj}\left(x'_j - x'_i\right)$$
$$u'_2 = y'_{pj}\left(z'_j - z'_i\right) - z'_{pj}\left(y'_j - y'_i\right)$$
$$u'_3 = z'_{pj}\left(x'_j - x'_i\right) - x'_{pj}\left(z'_j - z'_i\right)$$
$$u'_4 = u'_1\left(y'_j - y'_i\right) - u'_3\left(z'_j - z'_i\right) \tag{29}$$
$$u'_5 = u'_2\left(z'_j - z'_i\right) - u'_1\left(x'_j - x'_i\right)$$
$$u'_6 = u'_3\left(x'_j - x'_i\right) - u'_2\left(y'_j - y'_i\right)$$

$$N' = \left(u'^2_1 + u'^2_2 + u'^2_3\right)^{\frac{1}{2}}$$

$$L'_1 = S_{1i}\cos\theta'_{ij}\sin\varphi'_{ij} + 0.25S_{2i}\sin 2\theta'_{ij}\sin 2\varphi'_{ij}$$
$$L'_2 = S_{1i}\cos^2\theta'_{ij}\cos\varphi'_s - S_{2i}\sin\theta'_{ij}\sin^2\varphi'_{ij}$$
$$L'_3 = u'_2\cos\theta'_j\cos\varphi'_j + u'_3\cos\theta'_j\sin\varphi'_j - u'_1\sin\theta'_j$$
$$L'_4 = -u'_2\sin\varphi'_j + u'_3\cos\varphi'_j \tag{30}$$
$$L'_5 = u'_4\cos\theta'_j\cos\varphi'_j + u'_5\cos\theta'_j\sin\varphi'_j - u'_6\sin\theta'_j$$
$$L'_6 = -u'_4\sin\varphi'_j + u'_5\cos\varphi'_j$$

$$X' = \left(1 - \sin^2\theta'_{ij}\cos^2\varphi'_{ij}\right)^{\frac{1}{2}} \tag{31}$$

Then the secondary scattered fields components in the moving frame can be written as

$$E'^{cs}_\theta = -\left[\frac{1}{X'^2 N'^2}\left(S_{1j}L'_3\left(L'_1 L'_3 + L'_2 L'_4\right)\right.\right.$$
$$\left.\left. + \frac{S_{2j}}{d'_{ij}}L'_4\left(L'_1 L'_5 + L'_2 L'_6\right)\right)\right]\frac{e^{jk'\left(d'_{ij}+r'_j\right)}}{k'^2 d'_{ij}r'_j} \tag{32}$$

$$E'^{cs}_\varphi = \left[\frac{1}{X'^2 N'^2}\left(-S_{1j}L'_4\left(L'_1 L'_3 + L'_2 L'_4\right)\right.\right.$$
$$\left.\left. + \frac{S_{2j}}{d'_{ij}}L'_3\left(L'_1 L'_5 + L'_2 L'_6\right)\right)\right]\frac{e^{jk'\left(d'_{ij}+r'_j\right)}}{k'^2 d'_{ij}r'_j} \tag{33}$$

Referring Equation (13) for transforming scattered fields back into the stationary frame, the time-harmonic field components can be expressed as

$$E^{cs}_\theta = -\frac{\sqrt{1-\beta^2}}{1-\beta\cos\theta_j}\left[\frac{1}{X'^2 N'^2}(S_{1j}L'_3(L'_1 L'_3 + L'_2 L'_4)\right.$$
$$\left. + \frac{S_{2j}}{d'_{ij}}L'_4(L'_1 L'_5 + L'_2 L'_6))\right]\frac{e^{jk'\left(d'_{ij}+r'_j-ct'\right)}}{k'^2 d'_{ij}r'_j} \tag{34}$$

$$E^{cs}{}_{\varphi} = -\frac{\sqrt{1-\beta^2}}{1-\beta\cos\theta_j}\left[\frac{1}{X'^2 N'^2}(S_{1j}L'_4(L'_1 L'_3 + L'_2 L'_4)\right.$$

$$\left. -\frac{S_{2j}}{d'_{ij}}L'_3(L'_1 L'_5 + L'_2 L'_6))\right]\frac{e^{jk'(d'_{ij}+r'_j-ct')}}{k'^2 d'_{ij} r'_j} \qquad (35)$$

Considering t'_{ij} and t'_j the corresponding elapsed times for d'_{ij} and r'_j, respectively; it can be written that

$$t' = \tau' + t'_{ij} + t'_j \qquad (36)$$

$$jk'(d'_{ij} + r'_j - ct') = -jk'c\tau\sqrt{1-\beta^2} \qquad (37)$$

Applying Equations (9), (24) and (37) to Equations (34) and (35) leads to the time-harmonic secondary scattered fields in the stationary frame

$$E^{cs}{}_{\theta} = -\frac{(1-\beta^2)^{\frac{5}{2}}}{(1-\beta\cos\theta_{ij})(1-\beta\cos\theta_j)^2}$$

$$\left[\frac{1}{X'^2 N'^2}(S_{1j}L'_3(L'_1 L'_3 + L'_2 L'_4)\right. \qquad (38)$$

$$\left. +\frac{S_{2j}}{d'_{ij}}L'_4(L'_1 L'_5 + L'_2 L'_6))\right]\frac{e^{-jkc\tau}}{k^2 d_{ij} r_j}$$

$$E^{cs}{}_{\varphi} = \frac{(1-\beta^2)^{\frac{5}{2}}}{(1-\beta\cos\theta_{ij})(1-\beta\cos\theta_j)^2}$$

$$\left[\frac{1}{X'^2 N'^2}(S_{1j}L'_4(L'_1 L'_3 + L'_2 L'_4)\right. \qquad (39)$$

$$\left. -\frac{S_{2j}}{d'_{ij}}L'_3(L'_1 L'_5 + L'_2 L'_6))\right]\frac{e^{-jkc\tau}}{k^2 d_{ij} r_j}$$

$$\vec{H}^{cs} = \frac{1}{\eta}\hat{r}_j \times (E_\theta^{cs}\hat{\theta} + E_\varphi^{cs}\hat{\varphi}) \qquad (40)$$

It is important to notice that components of these fields represent secondary scattered fields in the observation point at time $t = \tau + \frac{d_{ij}+r_j}{c}$.

The developed approach for deriving direct and coupling scattered fields can be generalized to a collection of arbitrary number of spheres by the employment of an iterative procedure to achieve the scattered fields up to the second order. This is a good approximation regarding that the spheres are in the farfield of each other, than the amplitudes of scattered fields more than second order are negligible.

3 | NUMERICAL RESULTS

Theoretical results achieved in the last section for a collection of both stationary and moving spheres are simulated to have a deeper physical insight into the problem. The incident field is considered to propagate in the negative $\hat{x}$ direction $(\vec{E}^i = e^{-jkx}\hat{y})$ and the maximum value used for n in the Mie theory is set to be 100 to calculate the numerical results. The azimuth and elevation angles are angular measurements in the spherical coordinate system and have intervals of $[0,2\pi]$ and $[0, \pi]$, respectively.

3.1 | Fields for stationary scatterers

In this section the refractive index of the spheres is set to be $n = 3.2+j0.32$. An individual stationary sphere with a radius of $a = 1$ cm and size parameter of $ka = 10$ ($f = 47.75$ GHz) which is located at $(x, y, z)=(0, -5m, 0)$ is considered. Figure 4(a) represents the three-dimensional (3D) scattered field pattern at a distance of 10 m from the origin of the coordinate system (radius $r = 10$ m) and - Figure 4(b) illustrates the azimuth pattern for a 90° elevation angle. According to the position of the sphere, it is expected for the elevation pattern to be symmetric about the elevation angle of 90° which is confirmed by Figure 4(c).

In the following, scattered fields are calculated for two similar spheres with $a = 5$ mm and $ka = 1.5$ ($f = 14.3$ GHz) which are located at (1.5 cm, 1.5 cm, 0) and (−1.5 cm, −1.5 cm, 0). Figure 5(a) shows the field pattern at $r = 10$ m and the two-dimensional (2D) patterns in the azimuth and elevation planes are illustrated in Figures 5(b,c), respectively. Figure 5(b) demonstrates that the maximum level for coupling fields are approximately around the azimuth angle of 225° which is expected regarding the position of the spheres and direction of the incident field. Figure 5(c) again has the property of symmetry due to the position of spheres.

Ten similar spheres with $a = 5$ mm and $ka = 3$ ($f = 28.6$ GHz) with locations shown in Table 1 are considered and the bistatic scattered field pattern at $r = 20$ m is illustrated in Figure 6(a). Maximum amplitude in both Figures 6(a,b) occurs around azimuth angle of 180° which states the effect of the addition of direct scattered fields. Maximum deviations of the first and second-order fields, which happen at about 45°,225° as highlighted, are due to the coupling interactions regarding the locations of spheres. These deviations show the importance of the coupling fields when the number of spheres increases. Figure 6(c) is also symmetric about the elevation angle of 90°.
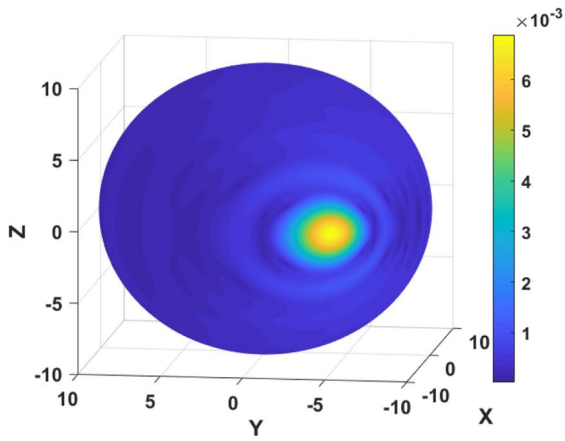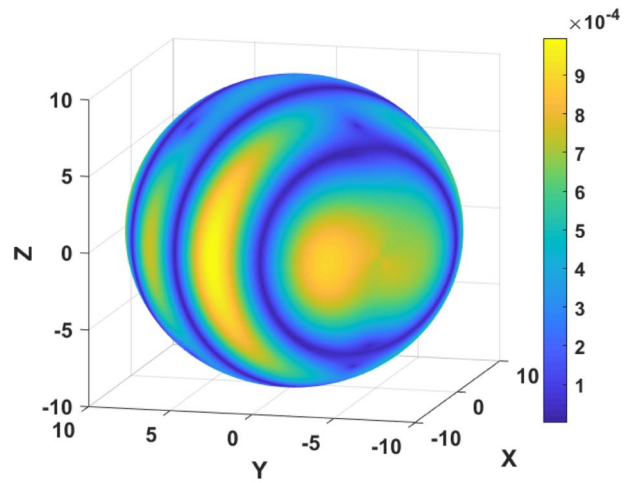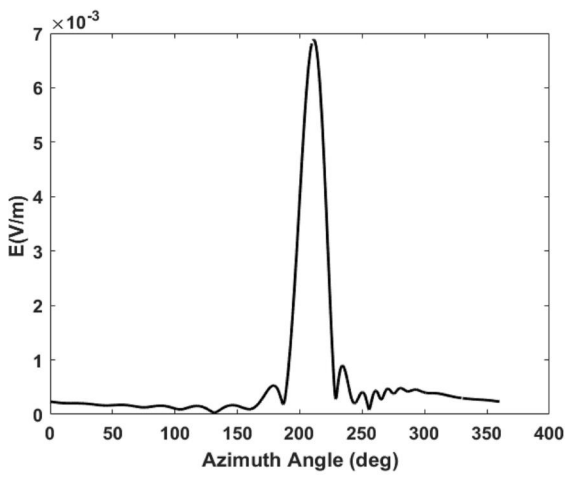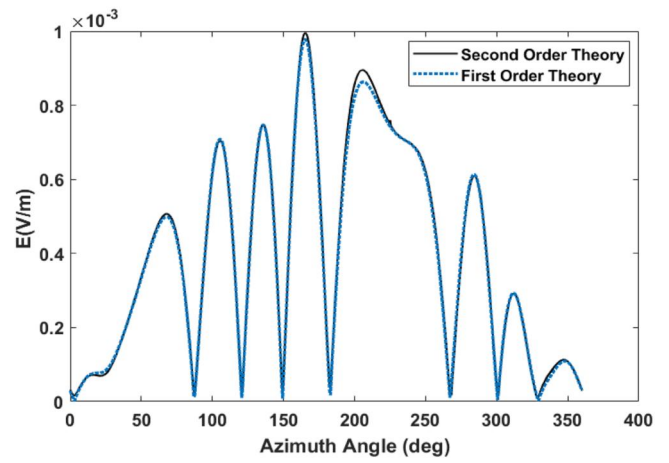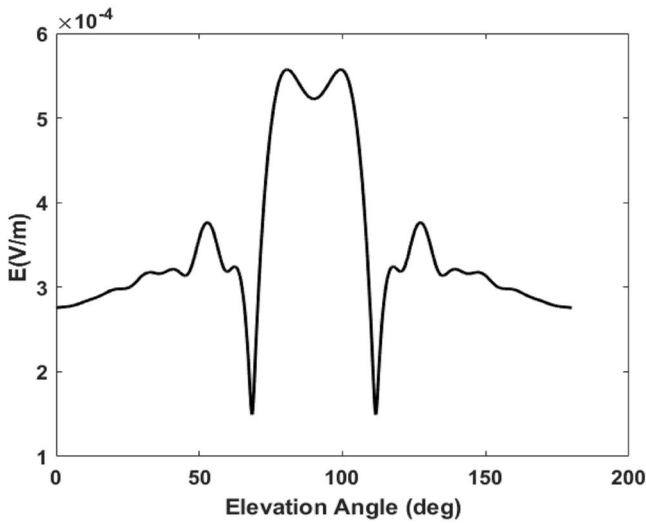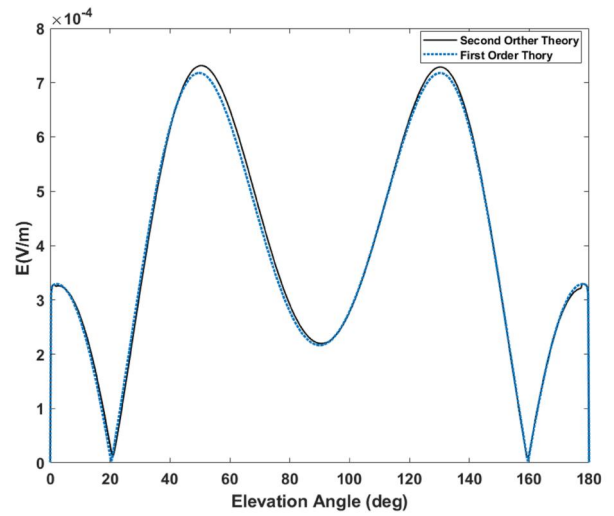
FIGURE 4 (a) Electric scattered field pattern for a stationary sphere at $r = 10$ m. (b) Bistatic scattered field amplitude for an elevation angle of $\pi/2$. (c) Bistatic scattered field amplitude for an azimuth angle of π

FIGURE 5 (a) Electric scattered field pattern for two stationary spheres at $r = 10$ m. (b) Bistatic scattered field amplitude for an elevation angle of $\pi/2$. (c) Bistatic scattered field amplitude for an azimuth angle of π

TABLE 1 Configurations of ten stationary spheres

No	x (cm)	y (cm)	z (cm)
1	1.5	1.5	0
2	4.5	4.5	0
3	7.5	7.5	0
4	10.5	10.5	0
5	13.5	13.5	0
6	−1.5	−1.5	0
7	−4.5	−4.5	0
8	−7.5	−7.5	0
9	−10.5	−10.5	0
10	−13.5	−13.5	0

3.2 | Fields for moving scatterers

In this section, the amplitude of the scattered electric field is illustrated in a determined observation point with respect to the time. The influence of the effective parameters such as the size, material, number, velocity, position of the spheres and the frequency of the incident wave on the scattered fields of the moving spheres has been demonstrated in this section. According to the quick time varying phase of the both primary and secondary scattered fields, it is expected that the field patterns appear with a slowly varying amplitude envelop with a rapidly varying carrier.

Firstly, one sphere with $a = 1$ mm, $ka = 10$ ($f = 477$ GHz), $n = 3.2 + j0.32$ and initial position in the origin of the coordinate system, moving with the velocity of $v = 0.5$ m/s is considered. The scattered field amplitude in the observation point of $(x_p, y_p, z_p) = (-5$ m, 0, 5 m) is illustrated in Figure 7. According to the speed of the sphere and height of the observation point, it is expected that the maximum level of field amplitude occurs at about $t = 10$ s revealing that the forward scattering is dominant for this ka value. Since the position of the sphere is symmetric about the observation point, scattered field amplitude must be either symmetric which is in full agreement with Figure 7.

In the next step, the conditions are the same as the previous sphere except that the velocity is set to $v = 2 \times 10^8$ m/s. As can be seen in Figure 8, the amplitudes before the peak moment (t_{peak}) are larger than their symmetric corresponding moments (after t_{peak}) which is because of the effect of aberration in the propagation direction phenomenon. Also, the peak amount of the amplitude is decreased compared with the previous condition.

For two spheres scenario, a reference mode is considered and only one parameter would be changed in each following mode to have a better understanding of the intended parameter. In the reference mode, two spheres are assumed to have $a = 1$ mm, $v = 1$ m/sand $n = 3.2 + j0.32$. The size parameter is set to $ka = 10$ ($f = 477$ GHz) and coordinates of observation
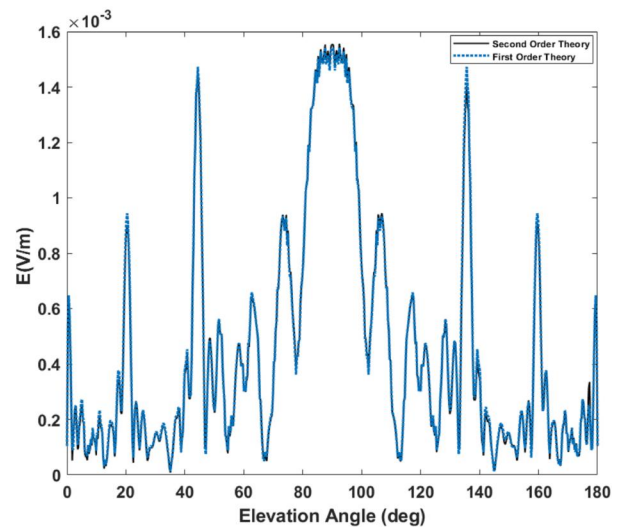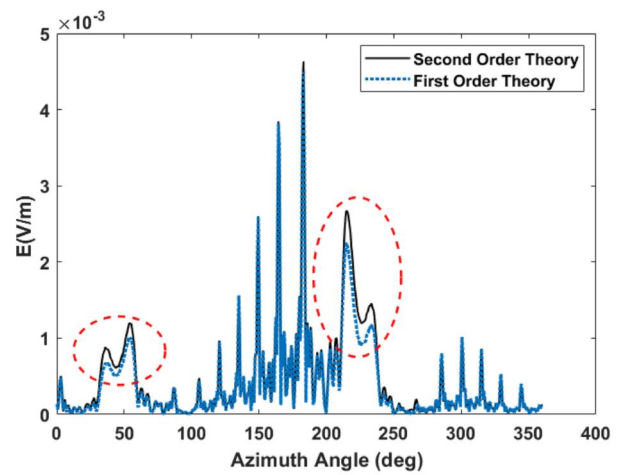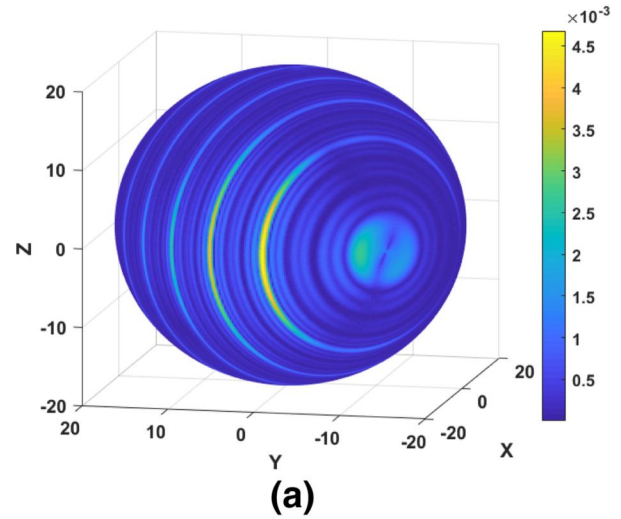

(a)

(b)

(c)

FIGURE 6 (a) Electric scattered field pattern for 10 stationary spheres at $r = 20$ m. (b) Bistatic scattered field amplitude for an elevation angle of $\pi/2$. (c) Bistatic scattered field amplitude for an azimuth angle of π.
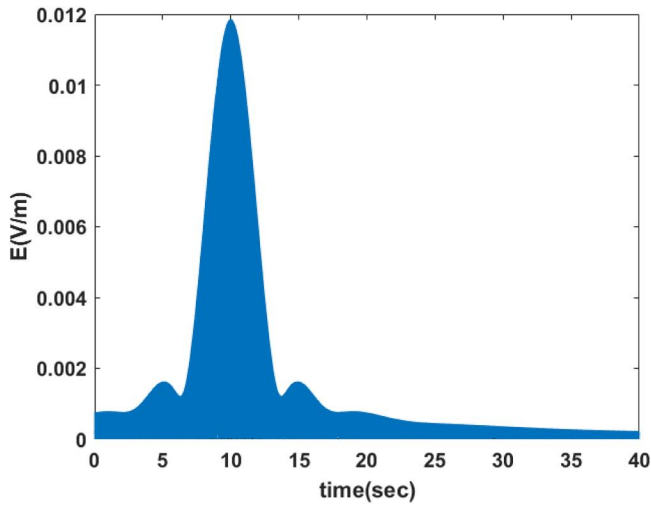
FIGURE 7 Time-domain electric scattered field amplitude for a moving sphere
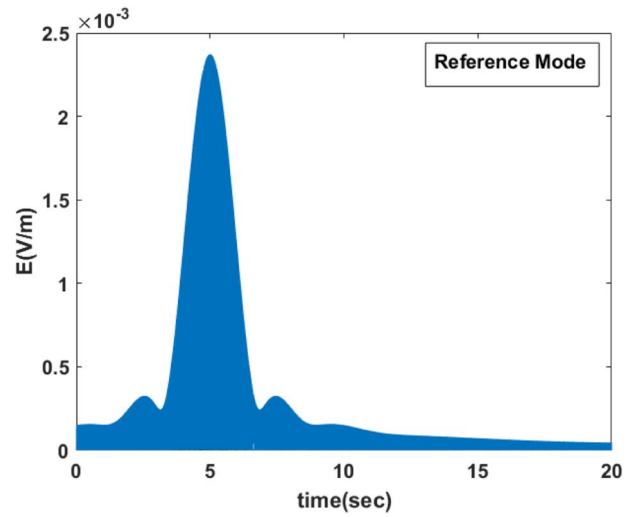

FIGURE 9 Time-domain electric scattered field amplitude for a moving sphere (reference mode)
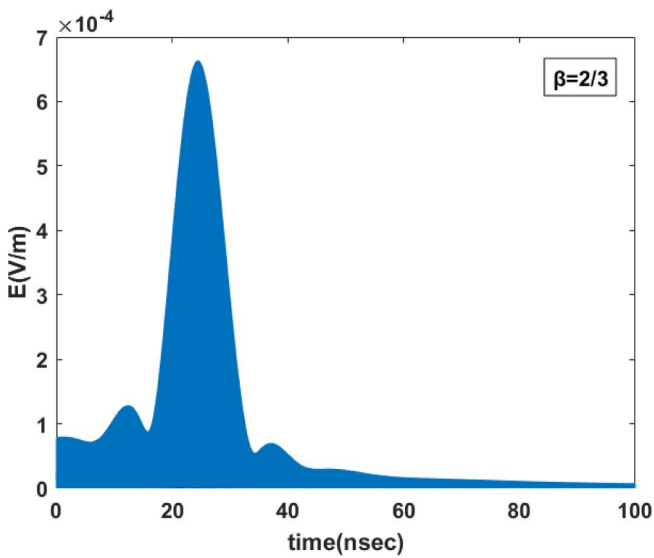

FIGURE 8 Time-domain electric scattered field amplitude for a moving sphere ($\beta = 2/3$)
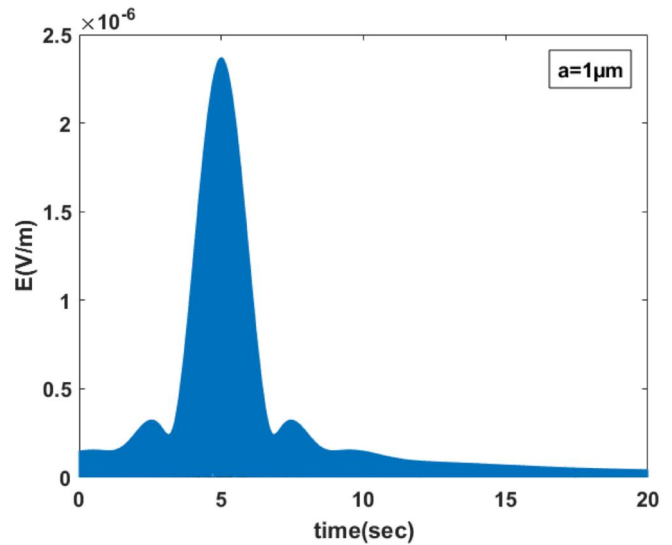

FIGURE 10 Time-domain electric scattered field amplitude for two moving spheres ($a = 1$ μm)

TABLE 2 Configurations of reference mode for two moving spheres (units in m)

Observation point			Sphere 1			Sphere 2		
x_p	y_p	z_p	x_1	y_1	z_1	x_2	y_2	z_2
−5	0	5	0	−0.01	0	0	0.01	0

point and primary location of spheres are given in Table 2. The maximum amplitude at $t = 5$ s and symmetry in Figure 9 could be predicted by physical interpretation. The peak at $t = 5$ s is about two times the peak shown in Figure 7 which indicates that the direct scattered field of each sphere has been added constructively.

This time, the radius of the spheres is changed to $a = 1$ μm and Figure 10 shows that the amplitude reduction of the scattered field (about 1000 times) is proportional to the reduction of the radiuses. Figure 11 relates to the mode $ka = 5$. Thus comparing this with the results of the reference mode reveals that the lower ka causes a wider beam, which is in agreement with the general fact that moving from optical through Mie and Rayleigh scattering regions makes scattering pattern more homogeneous then forward scattered pattern becomes wider.

In the next mode to represent the effect of the dielectric material, the extinction coefficient is omitted and the refractive index is set to be $n = 3.2$, as shown in Figure 12.
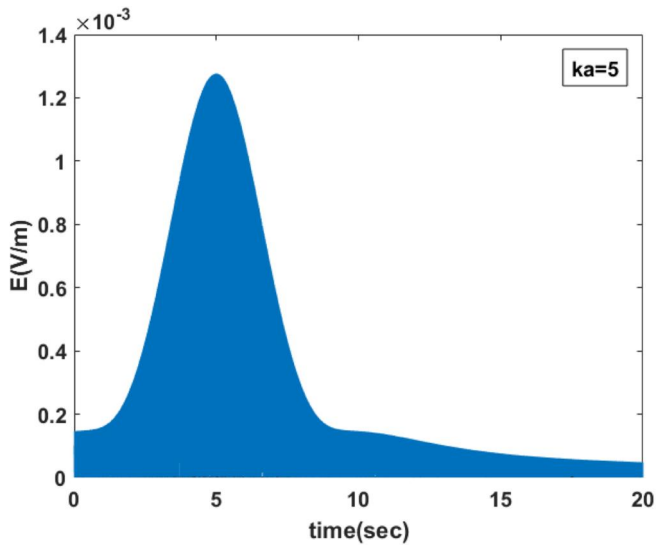
FIGURE 11 Time-domain electric scattered field amplitude for two moving spheres ($ka = 5$)
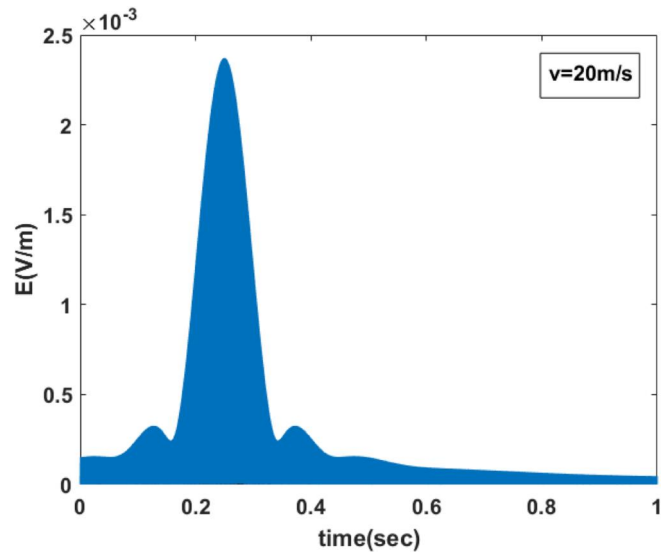

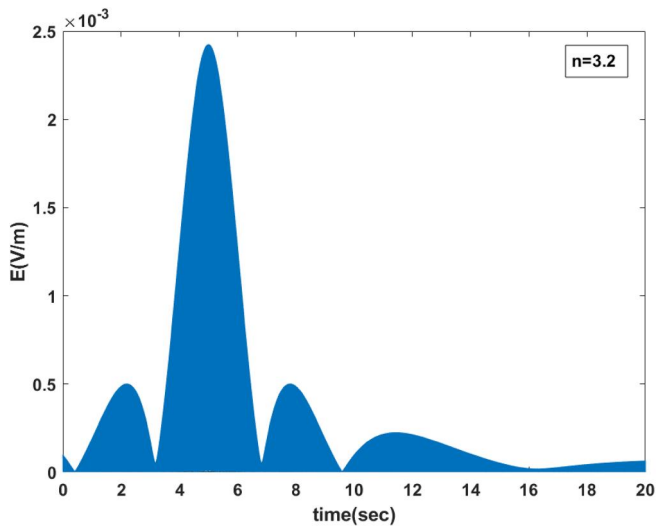**FIGURE 13** Time-domain electric scattered field amplitude for two moving spheres ($v = 20$ m/s)

FIGURE 12 Time-domain electric scattered field amplitude for two moving spheres ($n = 3.2$)
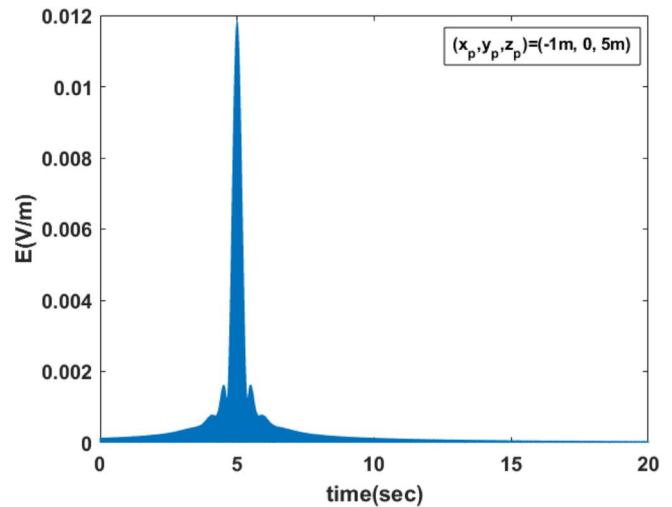

FIGURE 14 Time-domain electric scattered field amplitude for two moving spheres with (x_p, y_p, z_p)=(-1 m, 0, 5 m)

Figure 13 is for a condition that spheres move with the velocity of $v = 20$ m/s which states that the pattern has been scaled. Since the velocity of spheres is negligible when compared with the velocity of light, the electric scattered field amplitude is similar to the reference mode.

In the next situation, the observation point is approached to (x_p, y_p, z_p)=(-1 m, 0, 5 m), as shown in Figure 14, which means that the closer distances result in narrower scattered beam-widths.

Next, the velocity is set to $v = 2 \times 10^8$ m/s. As depicted in Figure 15, the scattered electric field amplitude is going to be more asymmetric by increasing the velocity to the relativistic speeds due the aberration in the propagation direction

phenomenon. Also, the peak amplitude decreases compared with the previous and reference mode.

In the following, scattered field amplitude for a collection of ten moving spheres with $a = 1$ mm and $v = 1$ m/s is calculated. The size parameter and the refractive index are set to be $ka = 10$ ($f = 477$ GHz) and $n = 3.2+j0.32$, respectively. Table 3 specifies the configuration of the spheres collection and the observation point is considered to be (x_p, y_p, z_p)=(-1 m, 0, 20 m). Figure 16 demonstrates the resulting scattered field amplitude.

Finally, time-domain electric scattered field amplitude for a collection of ten spheres moving in relativistic speed ($\beta = 2/3$) is represented in Figure 17. The remaining parameters are the same as in the previous case.
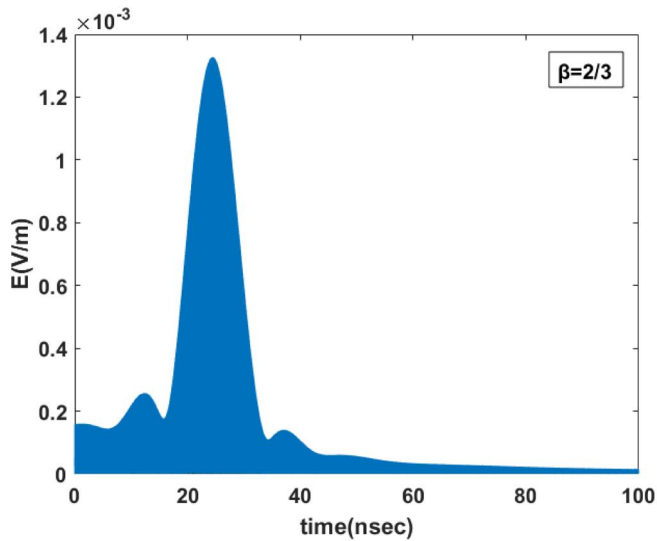
FIGURE 15   Time-domain electric scattered field amplitude for two moving sphere ($\beta = 2/3$)

TABLE 3   Configurations of ten moving spheres

No	x (cm)	y (cm)	z (m)
1	1.5	1.5	2
2	4.5	4.5	4
3	7.5	7.5	6
4	10.5	10.5	8
5	13.5	13.5	10
6	−1.5	−1.5	−2
7	−4.5	−4.5	−4
8	−7.5	−7.5	−6
9	−10.5	−10.5	−8
10	−13.5	−13.5	−10

4 | CONCLUSION

In this work, the Frame-Hopping Method (FHM) which is based on the STR is used to obtain time-domain relativistic scattered fields up to the second-order from an arbitrary collection of uniformly translational moving lossy-dielectric spheres. To gain a deeper physical insight into the problem, scattered fields for a collection of both stationary and moving spheres have been simulated. The influence of effective parameters such as the size, material, velocity, number, position of the spheres and also the frequency of the incident field on the scattered fields of a collection of moving spheres has been investigated and the obtained numerical results are in good agreement with physical concepts. Also, a wide variety of objects, such as raindrops, snowflakes and dust particles, could be approximated by spheres and the study of scattered fields from a collection of moving spheres has a substantial significance for many practical applications. The procedure applied in this work may be the basis for
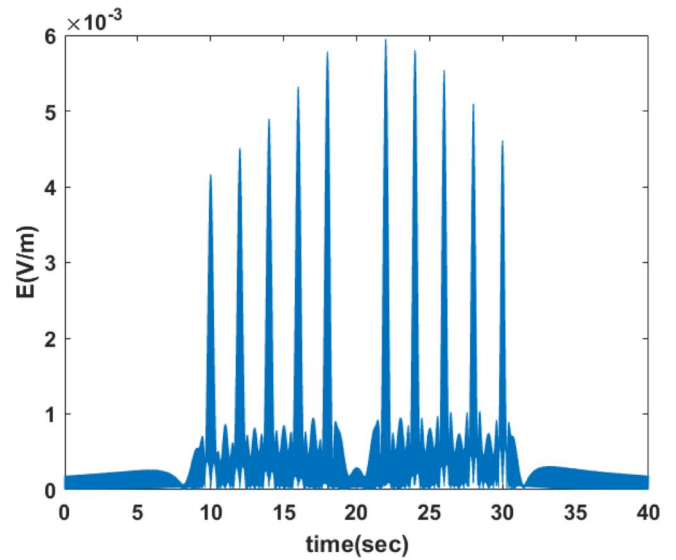

FIGURE 16   Time-domain electric scattered field amplitude for ten moving spheres
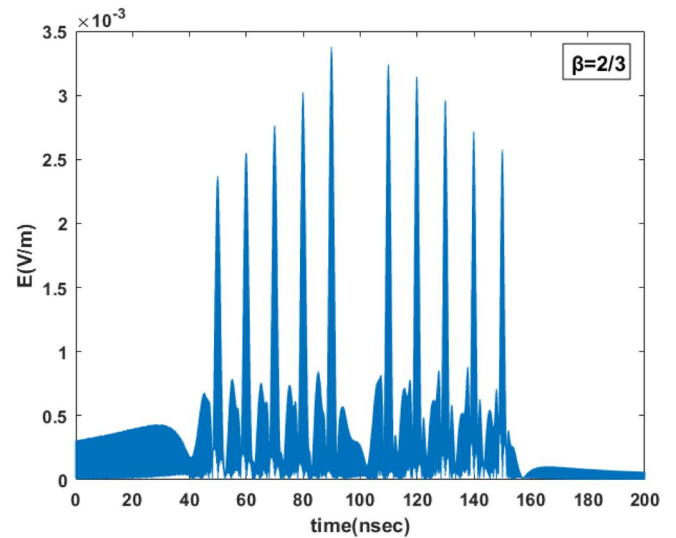

FIGURE 17   Time-domain electric scattered field amplitude for ten moving sphere ($\beta = 2/3$)

the study of multiple and random scattering from other collections of moving objects considering their mutual interactions.

REFERENCES

1. Hoang, T., Lazarian, A., Schlickeiser, R.: On origin and destruction of relativistic dust and its implication for ultrahigh energy cosmic rays. Astrophys. J. 806, 255 (2015)
2. Messiaen, A.M., Vandenplas, P.E.: High-frequency effect due to the axial drift velocity of a plasma column. Phys. Rev. 149(1), 131–140 (1966)
3. Yeh, C.: Scattering obliquely incident microwaves by a moving plasma column. J. Appl. Phys. 40(13), 5066–5075 (1969)
4. Shiozawa, T., Seikai, S.: Scattering of electromagnetic waves from an inhomogeneous magnetoplasma column moving in the axial direction. IEEE Trans. Antennas Propag. AP-20(4), 455–463 (1972)
5. Yan, Y.: Mass flow measurement of bulk solids in pneumatic pipelines. Meas. Sci. Technol. 7(12), 1687–1706 (1996)

6. Einstein, A.: Zur Elektrodynamik bewegter Körper. Annalen der Physik. 322(10), 891–921 (1905)

7. Sommerfeld, A.: Electrodynamics. Academic Press, New York (1952)

8. Pauli, W.: Theory of Relativity. Macmillan, New York (1958)

9. Yeh, C.: Reflection and transmission of electromagnetic waves by a moving dielectric medium. J. Appl. Phys. 36(11), 3513–3517 (1965)

10. Van, B.J.: Relativity and Engineering. Springer-Verlag, Berlin (1984)

11. Lee, S.W., Mittra, R.: Scattering of electromagnetic waves by a moving cylinder in free space. Canadian J. Phys. 45, 2999–3007 (1967)

12. Censor, D.: Scattering of electromagnetic waves by a cylinder moving along its axis. Microw. Theory Techn. 17, 154–158 (1969)

13. Le Vine, D.M.: Scattering from a moving cylinder, oblique incidence. Radio Sci. 15, 497–504 (1973)

14. Freni, A., Mias, C., Ferrari, R.L.: Finite element analysis of electromagnetic wave scattering by a cylinder moving along its axis surrounded by a longitudinal corrugated structure. IEEE Trans. Magnetics. 32(3), 874–877 (1996)

15. Pastorino, M., Raffetto, M.: Scattering of electromagnetic waves from a multilayer elliptic cylinder moving in the axial direction. IEEE Trans. Antennas Propag. 61(9), 4741–4753 (2013)

16. Restrick, R.C.: 111, Electromagnetic scattering by a moving conducting sphere. Radio ScL. 3(12), 1144–1157 (1968). new series

17. Lakhtakia, A., Varadan, V.V., Varadan, V.K.: Plane wave scattering response of a simply moving electrically small, chiral sphere. J. Mod. Opt. 38, 1841–1847 (1991)

18. Shiozawa, T.: Electromagnetic scattering by a moving small panicle. J. Appl. Phys. 39, 293–297 (1968)

19. Cooper, J.: Scattering of electromagnetic fields by a moving boundary: The one-dimensional case. IEEE Trans. Antennas Propag. 28(6), 791–795 (1980)

20. Chrissoulidis, D., Kriezis, E.: The scattering behavior of a slightly rough surface moving parallel to its mean plane with uniform velocity. IEEE Trans. Antennas Propag. 33(7), 793–796 (1985)

21. Tzikas, A.A., Chrissoulidis, D.P., Kriezis, E.E.: Relativistic bistatic scattering by a uniformly moving random rough surface. IEEE Trans. Antennas Propag. AP-34, 1046–1052 (1986)

22. Ott, R.H., Hufford, G.: Scattering by an arbitrarily shaped conductor in uniform motion relative to the source of an incident spherical wave. Radio Sci. 3, 857–861 (1968)

23. Twersky, V.: Relativistic scattering of electromagnetic waves by moving obstacles. J. Math Phys. 12(11), 2328–2341 (1971)

24. Abdelazeez, M., Peach, L.C., Borkar, S.R.: Scattering of electromagnetic waves from moving surfaces. IEEE Trans. Antennas Propag. 27(5), 679–684 (1979)

25. De Zutter, D.: Fourier analysis of the signal scattered by objects in translational motion, part I and II. Appl. Sci. Res. 36, 169–241 (1980)

26. Michielsen, B.L., et al.: Three-dimensional relativistic scattering of electromagnetic waves by an object in uniform translation motion. J. Math. Phys. 22, 2716–2722 (1981)

27. De Cupis, P., Gerosa, G., Schettini, G.: Electromagnetic scattering by an object in relativistic translational motion. J. Electromagn. Waves Appl. 14, 1037–1062 (2000)

28. De Cupis, P., et al.: Electromagneticwave scattering by a perfectly conducting wedge in uniform translational motion. J. Electromagn. Waves Appl. 16, 345–364 (2002)

29. Ciarkowski, A.: Scattering of an electromagnetic pulse by a moving wedge. IEEE Trans. Antennas Propag. 57, 688–693 (2009)

30. Idemen, M., Alkumru, A.: Relativistic scattering of a plane-wave by a uniformly moving half-plane. IEEE Trans. Antennas Propag. 13, 3429–3440 (2006)

31. Ciarkowski, A.: Electromagnetic pulse diffraction by a moving halfplane. PIER. 64, 53–67 (2006)

32. Rosa, G.S., Nicolini, J.L., Hasselman, F.J.V.: Relativistic aspects of plane wave scattering by a perfectly conducting half-plane with uniform velocity along an arbitrary direction. IEEE Trans. Antennas Propag. 65(9), 4759–4767 (2017)

33. Garner, T.J., et al.: Lorentz invariance of absorption and extinction cross sections of a uniformly moving object. Phys. Rev. 96(5), 053839 (2017)

34. Garner, T.J., et al.: Scattering characteristics of relativistically moving concentrically layered spheres. Phys. Lett. 382(5), 362–366 (2018)

35. Garner, T.J., et al.: Time-domain electromagnetic scattering by a sphere in uniform translational motion. JOSA A. 34(2), 270–279 (2017)

36. Harfoush, F., Taflove, A., Kriegsman, G.A.: A numerical technique for analyzing electromagnetic wave scattering from moving surfaces in one and two dimensions. IEEE Trans. Antennas Propag. 37, 55–63 (1989)

37. Ho, M.: Numerical simulation of scatting of electromagnetic waves from traveling and/or vibrating perfect conducting planes. IEEE Trans. Antennas Propag. 54(1), 152–156 (2006)

38. Kuang, L., et al.: Relativistic FDTD analysis of far-field scattering of a high-speed moving object. IEEE Antennas Wirel. Propag. Lett. 14, 879–882 (2015)

39. Zheng, K.S., et al.: Electromagnetic properties from moving dielectric in high speed with Lorentz-FDTD. IEEE Antennas Wirel. Propag. Lett. 15, 934–937 (2016)

40. Shao, J.H., Ma, X.K., Kang, Z.: Numerical analysis of electromagnetic scattering from a moving target by the Lorentz precise integration time-domain method. IEEE Trans. Antennas Propag. 65(10), 5649–5653 (2017)

41. Zheng, K.S., et al.: Analysis of scattering fields from moving multi-layered dielectric slab illuminated by an impulse source. IEEE Antennas Wirel. Propag. Lett. 16, 2130–2133 (2017)

42. Shao, J, Ma, X., Wang, J.: A numerical method without coordinate transformations to the electromagnetic problem involving objects in arbitrary translational motion. IEEE Trans. Antennas Propag. 66(8), 4158–4169 (2018)

43. van de Hulst, H.C.: Light Scattering by Small Particles. Dover, New York (1981)

44. Bohren, C.F., Huffman, D.R.: Absorption and Scattering of Light by Small Particles (1983)

45. Kong, J., Tsang, L., Ding, K.: Scattering of Electromagnetic Waves: Theories and Applications, vol. 1. Wiley, New York (2000)

46. Kerker, M.: The Scattering of Light. Academic, New York (1969)

47. De Zutter, D.: Scattering by a rotating dielectric sphere. IEEE Trans. Antennas Propag. AP-28, 643–651 (1980)

48. Tanaka, K.: Scattering of electromagnetic waves by a rotating perfectly conducting cylinder with arbitrary cross section: Point-matching method. IEEE Trans. Antennas Propag. 28(6), 796–803 (1980)

49. Zutter, D.D.: Scattering by a rotating circular cylinder with finite conductivity. IEEE Trans. Antennas Propag. 31(1), 166–169 (1983)

50. De Zutter, D., Goethals, D.: Scattering by a rotating conducting sphere. IEEE Trans. Antennas Propagat. 32, 95–98 (1984)

51. Kleinman, R.E., Mack, R.B.: Scattering by linearly vibrating objects. IEEE Trans. Antennas Propag. 27(3), 344–352 (1979)

52. Van Bladel, J., De Zutter, D.: Reflections from linearly vibrating objects: Plane mirror at normal incidence. IEEE Trans. Antennas Propag. AP-29, 629–636 (1981)

53. De Zutter, D.: Reflections from linearly vibrating objects: plane mirror at oblique incidence. IEEE Trans. Antennas Propag. 30(5), 898–903 (1982)

54. Lawrence, D.E., Sarabandi, K.: Electromagnetic scattering from vibrating penetrable objects using a general class of time-varying sheet boundary conditions. IEEE Trans. Antennas Propag. 54(7), 2054–2061 (2006)